Synthetic and Systems Biotechnology 4 (2019) 165–172

Contents lists available at ScienceDirect

Synthetic and Systems Biotechnology

journal homepage: http://www.keaipublishing.com/synbio

Detailed profiling of carbon fixation of *in silico* synthetic autotrophy with reductive tricarboxylic acid cycle and Calvin-Benson-Bassham cycle in *Escherichia coli* using hydrogen as an energy source

Hsieh-Ting-Yang Cheng[a], Shou-Chen Lo[b], Chieh-Chen Huang[b,d,e], Tsung-Yi Ho[a], Ya-Tang Yang[c,*]

[a] Department of Computer Science, National Tsing Hua University, Hsinchu, 30013, Taiwan, R.O.C
[b] Department of Life Sciences, National Chung-Hsing Univeristy, Taichung, Taiwan, R.O.C
[c] Department of Electrical Engineering, National Tsing Hua University, Hsinchu, 30013, Taiwan, R.O.C
[d] Program in Microbial Genomics, National Chung Hsing University, Taichung, Taiwan, R.O.C
[e] Innovation and Development Center of Sustainable Agriculture, National Chung Hsing University, Taichung, Taiwan, R.O.C

ARTICLE INFO

Keywords:
Reductive tricarboxylic acid cycle
Calvin-Benson-Bassham cycle
Carbon fixation
Metabolism

ABSTRACT

Carbon fixation is the main route of inorganic carbon in the form of CO_2 into the biosphere. In nature, RuBisCO is the most abundant protein that photosynthetic organisms use to fix CO_2 from the atmosphere through the Calvin-Benson-Bassham (CBB) cycle. However, the CBB cycle is limited by its low catalytic rate and low energy efficiency. In this work, we attempt to integrate the reductive tricarboxylic acid and CBB cycles *in silico* to further improve carbon fixation capacity. Key heterologous enzymes, mostly carboxylating enzymes, are inserted into the *Esherichia coli* core metabolic network to assimilate CO_2 into biomass using hydrogen as energy source. Overall, such a strain shows enhanced growth yield with simultaneous running of dual carbon fixation cycles. Our key results include the following. (i) We identified two main growth states: carbon-limited and hydrogen-limited; (ii) we identified a hierarchy of carbon fixation usage when hydrogen supply is limited; and (iii) we identified the alternative sub-optimal growth mode while performing genetic perturbation. The results and modeling approach can guide bioengineering projects toward optimal production using such a strain as a microbial cell factory.

Introduction

Carbon fixation is the main route of inorganic carbon in the form of CO_2 into the biosphere. Photoautotrophs such as plants, algae and cyanobacteria fix about 300 gigatons of CO_2 from the atmosphere annually through photosynthesis [1]. Six carbon fixation pathways in nature that assimilate CO_2 into cells have been identified and reviewed and the physiological roles of the central carboxylating enzymes have been discussed [2–4]. Efforts are also made to identify synthetic carbon fixation pathways using a computational approach [5,6]. In particular, Milo's group has searched over a database of ~5000 enzymes for possible carbon fixation pathways and analyzed their performance and thermodynamic feasibility [5]. Attempts from heterologous Ribulose 1,5-bisphosphate carboxylase/oxygenase (RuBisCO) expression to facilitate growth in *Escherichia coli* (*E. coli*) have been made [7–9] and reviewed [10]. Recently, Antonovsky, et al. have also created a non-native CBB cycle in *E. coli* to achieve hemi-autotrophic growth [11]. They employed adaptive laboratory evolution in xylose-limited chemostat to fine tune branching out of an intermediate metabolite in the CBB cycle to satisfy the kinetic requirements of the autocatalyic cycle [12]. Consequently, a fully-functional CBB pathway completely changes the trophic mode of *E. coli*. More importantly, the modularity of the design points to a direct path to replace the TCA-cycle-based energy module with energy harvesting molecular machinery [10]. A follow-up study elucidated the genetic basis and found the minimal set of mutations needed for a fully functional CBB cycle [13]. *In vitro* carbon fixation cycles with high kinetic rates under aerobic condition have also been demonstrated [14].

In nature, RuBisCO is the most abundant protein that photosynthetic organisms use to fix CO_2 from the atmosphere. The CBB cycle is often limited by its low catalytic rate but attempts to improve its performance have very marginal success [15,16]. In fact, the enzyme displays Pareto optimality with a trade-off between the enzyme catalytic rate and CO_2 specificity, possibly because of the difficulty in

Peer review under responsibility of KeAi Communications Co., Ltd.
* Corresponding author.
E-mail address: ytyang@ee.nthu.edu.tw (Y.-T. Yang).

https://doi.org/10.1016/j.synbio.2019.08.003
Received 4 June 2019; Received in revised form 6 August 2019; Accepted 19 August 2019

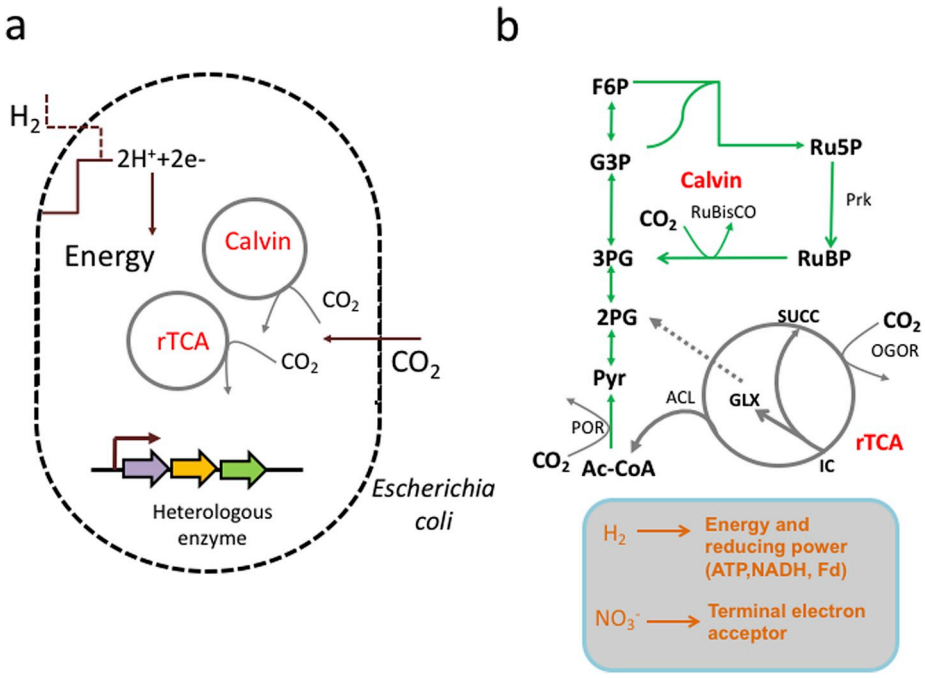

Fig. 1. Synthetic autotrophy of *Escherichia coli* with a dual carbon fixation cycle using hydrogen as source of energy. (a) Schematic of the configuration with both rTCA cyle and CBB cycle with CO_2 as the sole carbon source and H_2 as the energy source in *E. coli*. Heterologous enzymes are expressed to enact the non-native reductive TCA cycle and CBB cycles. (b) Schematic of *Escherichia coli* with hydrogen as source of energy. Both rTCA cyle with glyoxylate shunt and Calvin cycle are shown. Carboxylating enzymes including RuBisCO, POR, and OGOR. Only two key enzymes (Prk and RuBisCO) are needed for Calvin cycle. Only three key enzymes (POR, OGOR, and ACL) are needed for rTCA cycle. For clarity, only few compounds are shown in Calvin cycle. Glyoxylate is connected to 2 PG via glyoxylate assimilation pathway(Grey dash arrow). Hydrogen is oxidized to provide both energy and reducing power and nitrate is used as terminal electron acceptor. Abbreviations: Ac-CoA, acetyl-CoA; Pyr, pyruvate; 2 PG, D-glycerate-2-phophate; 3 PG, 3-Phospho-D-glycerate; G3P, glyceraldehyde-3-phosphate; IC, isocitrate; F6P, fructose-6- phosphate; GLX, glyoxylate; RuBP, ribulose-1-5-biphosphate; Ru5P, D-ribulose-5phosphate; SUCC, succinate; ACL, ATP citrate lyase; OGOR, 2-oxoglutarate:ferredoxin oxidoreductase; POR, pyruvate oxidoreductase; RuBisCO, ribulose 1,5-bisphosphate carboxylase/oxygenase; Prk, phosphoribulokinase; FR, favin reductase.

binding the featureless CO_2 molecules [16]. In this work, we address another naturally-existing carbon fixation cycle, namely the reductive tricarboxylic acid (TCA) cycle and attempt to integrate these two cycles into a single micro-organism, as shown in Fig. 1. In nature, the reductive TCA cycle plays a special role in carbon fixation because it is the most efficient pathway in terms of ATP consumption per CO_2 molecules fixed and runs near the thermodynamic edge [17].

In this study, we have chosen *E. coli* as it is still most genetically malleable micro-organism and the predicted strain can be readily realized using genetic engineering. We have chosen hydrogen as a convenient energy source, but the results obtained here can also be generalized to other energy sources. There are a few reasons to use hydrogen as an energy source. First, *E. coli* possesses innate hydrogenases that readily convert hydrogen to serve as reducing power and energy source of electrons for biosynthesis [18]. In comparison, to use light as an energy source, light harvesting machinery must be heterologously expressed, which is extremely challenging. Moreover, recent technological advances have enabled efficient electrosynthesis of hydrogen by combining semi-conductor based photovoltaic cells and highly efficient catalysts, which has made hydrogen a favorable and efficient energy source [19].

Constraint-based flux balance analysis has been extensively used to compute the growth yield and secretion of desired metabolic products [20,21]. To evaluate the feasibility of running a dual carbon fixation cycle, we identify and insert the necessary heterologous enzyme into a core metabolic network [22] and use constraint-based flux balance analysis to evaluate the resulting performance. We decided to use the core model instead of the genome-scale model of *E. coli*, as the core model is more generic and not too specific to *E. coli;* this may facilitate more general conclusions for other chassis microorganisms with similar central metabolisms. We employ constraint-based modeling to enable reliable predictions of how the CO_2 assimilation pathway integrates into the rest of the background metabolic network.

Materials and methods

The model

In this study, we insert heterologous enzymes into the *E. coli* core metabolism model [22]. Because key carboxylating enzymes and hygrogenase are oxygen-sensitive, we only consider *in silico* growth under anaerobic conditions. To complete the non-native CBB cycle, we investigate the recent hemi-autotrophy strain [11] and inserted RuBisCO and phosphoribulokinase (prk) enzymes. The kinase *prk* enables the phosphorylation of ribulose-5-phosphate to yield ribulose-1,5-bisphosphate (RuBP), the substrate of RuBisCO. Upon expression of *prk* and RuBisCO, ribulose-5-phosphate is readily phosphorylated to yield RuBP and is subsequently converted to 3-phosphoglycerate, which enables completion of the non-native CBB cycle. To completely reverse the existing TCA cycle, we identify two irreversible reactions within the TCA cycle and choose to insert 2-oxoglutarate:ferredoxin oxidoreductase (OGOR) and ATP citrate lyase (ACL). In addition, because pyruvate oxidoreductase (POR) is normally considered part of the reductive TCA cycle [3], we also insert it to maximize the overall potential capacity for carbon fixation. Because glyoxylate shunt is part of the TCA cycle in *E. coli*, we also include the glyoxylate assimilation pathway [23] via 2-phosphoglycerate (2 PG). Consequently, glyoxylate can be a potential cycle product from the combination of the rTCA cycle and anaplerotic reactions. 2 PG is the connecting intermediate from glyoxylate shunt to glyconeogenesis. ATP maintenance requirements for non-growth-associated maintenance (NGAM) and growth-associated maintenance (GAM) are also included. The core biomass objective function uses an NGAM of 8.39 mmol ATP/(gDW h) and a GAM of 59.81 mmol ATP/gDW.

Constraint-based flux balance analysis

The constraint-based flux balance is given by a linear optimization problem.

Maximize

$$Z = \mathbf{f}^T\mathbf{v}$$

Subject to

$$\mathbf{S}\cdot\mathbf{v} = 0$$

$$lb_i \le v_i \le ub_i$$

S is the stoichiometric matrix and **v** is the flux vector. $Z = \mathbf{f}^T\mathbf{v}$ is the objective function. lb_i and ub_i are the lower and upper bound of the ith component of the flux vector, **v**, respectively [20,21]. Flux balance analysis was used to compute the growth rate given a set of constraints on the bottleneck reaction. The COBRA toolbox is used to the solve linear optimization problem. The biomass reaction with coefficients from the literature [24] is also included and serves as the objective function. *In silico*, the network successfully assimilates CO_2 with the dual carbon fixation cycle.

Electron uptake reaction

In our model, we assume that hydrogen is used as an electron donor and nitrate is used as a terminal electron acceptor. The electron transport chain details are shown in Fig. 2. In the context of chemiosmotic theory, all these seemingly complicated reactions in the electron transport chain aim to generate excessive proton motive force for pumping protons out of cells to drive ATPase and various other energy-linked processes [24]. Overall, the necessary proton motive force is provided by a pair of reactions in the electron transport chain – hydrogen:menaquinone oxidoreductase and menaquinol:nitrate oxidoreductase. The reactions are given by

$$H_{2[e]} + 2H^+_{[c]} + \text{menaquinone}_{[c]} \text{ - > } 2H^+_{[e]} + \text{menaquinol}_{[c]} \quad (1)$$

$$NO_3^-{}_{[c]} + 2H^+_{[c]} + \text{menaquinol}_{[c]} \text{- > } NO_2^-{}_{[c]} + H_2O_{[c]} + 2H^+_{[e]} + \text{menaquinone}_{[c]} \quad (2)$$

where the subscripts [c] and [e] denote cellular and extracellular, respectively. The net result is four protons pumping out of the cell per hydrogen molecule. Assuming that ATP generation via ATPase has a stoichiometry of one ATP per four protons, one ATP is generated per hydrogen molecule.

For NADH generation, we hypothesize that reverse electron flow of the respiratory chain (NADH dehydrogenase) to reduce NAD. The reactions are

$$2H^+_{[e]} + NAD_{[c]} + \text{quinol}_{[c]} \text{ - > } 3H^+_{[c]} + NADH_{[c]} + \text{quinone}_{[c]} \quad (3)$$

$$NO_3^-{}_{[c]} + 2H^+_{[c]} + \text{quinone}_{[c]} \text{- > } NO_2^-{}_{[c]} + H_2O_{[c]} + 2H^+_{[e]} + \text{quinol}_{[c]} \quad (4)$$

Such a strategy of electron reversal is used by *E. coli* when the NADH supply is inadequate [24]. Additionally, we insert a heterologous enzyme or cytosolic or membrane-bound $NADP^+$-reducing hydrogenase [25–28] as the auxiliary electron pathway.

$$NADP_{[c]} + H_{2[c]} < - > NADPH_{[c]} + H^+_{[c]} \quad (5)$$

The reducing power via cofactor ferredoxin can be provided by favin reductase (FR), which converts reducing power from NADH.

$$FAD_{[c]} + NADH_{[c]} + 2H^+_{[c]} \text{- > } FADH_{2[c]} + NAD_{[c]} \quad (6)$$

Results

Profiling the autotrophic growth with hydrogen uptake

To understand the dual carbon fixation cycle, we fix the upper bound of flux of key enzymes – RuBisCO for the CBB cycle and OGOR and ACL for the rTCA cycle – as 1 $mmol.gDW^{-1}.hr^{-1}$. The growth rates for single and dual cycles as hydrogen uptake is varied are plotted in Fig. 3. The growth rate generally shows three distinct regions: (1) no growth, (2) hydrogen-limited state, and (3) carbon-limited state, as depicted in Fig. 3(b). The region of no growth is due to the failure of the energy supply to satisfy the ATP maintenance requirement. Beyond this region, as hydrogen increases, the growth rate shows a consistent increase until a plateau is reached. For simplicity, we plot one line in the hydrogen-limited state for Fig. 3(b), 3(c) and 3(d). In general, growth rate versus hydrogen curves could be multiple line segments in the region of hydrogen-limited state. Such multiple line segments indicate multiple phenotypes [21]. The region with a consistent increase and the plateau are identified as hydrogen-limited and carbon-limited states, respectively. At low hydrogen levels, the growth rate is limited by the hydrogen supply, which is a source of both energy and reducing power. When hydrogen is amply supplied, the growth rate is limited by the maximal flux of carboxylating enzymes. The efficiency difference

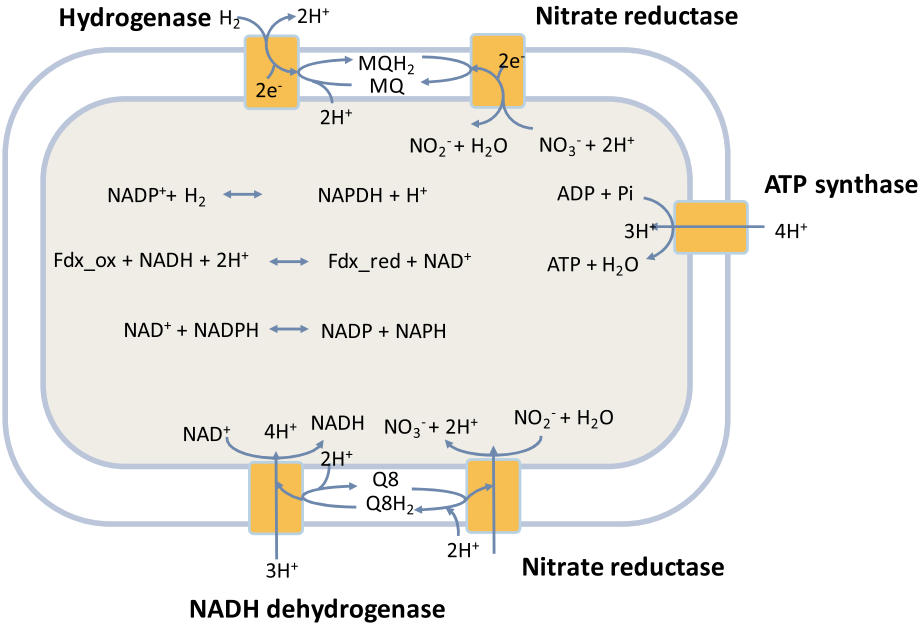

Fig. 2. Electron transport chain and cofactor generation using hydrogen as an energy source and reducing power. The enzymes on the cellular membrane are shown in bold. Abbreviations: Q8: ubiquinone, Q8H2: ubiquinol, MQ: menaquinone, MQH2: menaquinol.

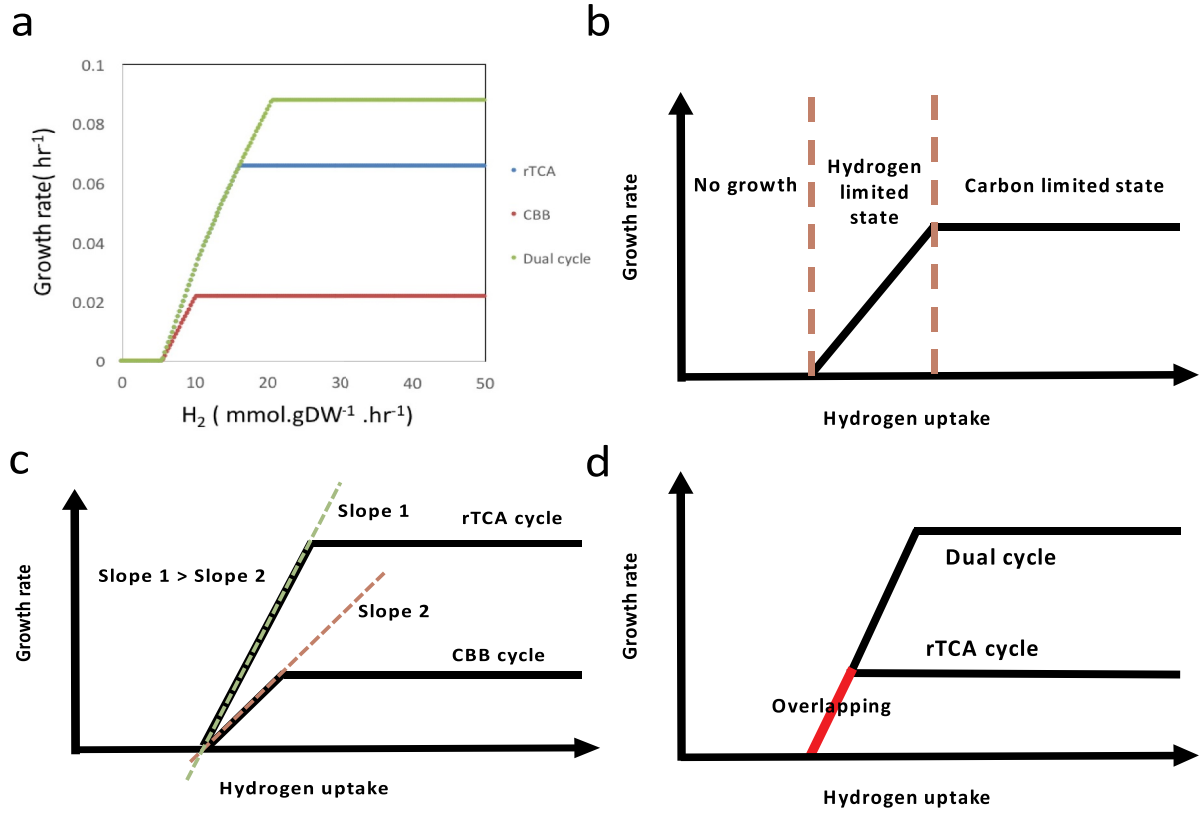

Fig. 3. Growth rate versus hydrogen uptake rate. (a) Computed growth rate varying hydrogen uptake rate. (b) Schematics of general features in growth rate plot showing three distinct regions: no growth, hydrogen-limited state, and carbon-limited state. (c) Schematics with exaggerated slope difference. The slope of the rTCA cycle is greater than that of the CBB cycle, which indicates that the rTCA cycle is more efficient in terms of ATP usage per CO_2 molecule fixed. (d) The overlapping of growth rate curves of rTCA and dual cycle indicates that only the rTCA cycle is running in this region.

between rTCA and CBB cycles is manifested in the different growth rates (biomass) with respect to hydrogen shown in Fig. 3(c). Note that the height of the plateau in Fig. 3(c) is related to the enzyme capacity of carboxylating enzymes, namely RuBisCO and OGOR. Equal enzyme capacity for RuBisCO and OGOR is assumed in Fig. 3(c). Close examination of the growth rate for dual and rTCA cycles reveals an overlapping region, shown in Fig. 3(d). In this overlapping region, only the rTCA cycle runs evenly, though both enzymes – RuBisCO and prk – are needed to run the CBB cycle. Henceforth, we establish that the growth rate versus hydrogen uptake shows a hierarchy of usage in the carbon fixation cycle. In other words, at low hydrogen levels, the rTCA cycle will be fully used with no carboxylation in the CBB cycle as it is more energetically favorable to run only on the rTCA cycle. When hydrogen is amply supplied, both cycles will be used to maximally supply carbon because the inorganic carbon supply becomes a limiting factor.

Profiling the autotrophic growth with flux of carboxylating enzymes

Next, we conduct the profiling while varying the flux of two key carboxylating enzymes, RuBisCO and OGOR. The growth rate versus flux of RuBisCO and OGOR at various hydrogen uptake levels is displayed in Fig. 4. At very low hydrogen uptake ($H_2 = -8$ mmol·gDW^{-1}hr^{-1}) corresponding to a hydrogen-limited state, there is a clear plateau in the region of dual carbon fixation, shown in Fig. 4(a). At very high hydrogen uptake ($H_2 = -50$ mmol· gDW^{-1}hr^{-1}) corresponding to a carbon-limited state, hydrogen is not a limiting factor for growth and there is no plateau. Profiling with hydrogen flux of carboxylating enzymes (Fig. 4) again shows two distinct states (carbon-limited and energy-limited). We can extend this distinction to different carboxylating enzyme capacity ratios and compare the maximal growth rate for single and dual cycles, as shown in Table 1. For the carbon-limited state ($H_2 = -50$ mmol.gDW^{-1}.hr^{-1}), when hydrogen is amply supplied, the growth rate of the dual cycle exceeds that of the single cycle. For the hydrogen-limited state ($H_2 = -8$ mmol.gDW^{-1}.hr^{-1}), the growth rate of dual cycle shows no enhancement compared with the single cycle when hydrogen is inadequately supplied.

Robustness analysis of dual carbon fixation

Varying a single parameter over a range of values and computing the objective for the linear optimization problem is termed robustness analysis [20,21]. Robustness analysis gives a much broader view of the optimal properties of a metabolic network. To demonstrate the usefulness of our strain, we can also carry out robustness analysis. In such a study, the upper bound of the selected reaction is varied and the corresponding growth rate is computed. For the data displayed in Fig. 5, we constrain the upper bound of RuBisCO, OGOR, and ACL reaction to 1 mmol·gDW^{-1}hr^{-1} for the central condition for the robustness study unless otherwise stated and the lower bound of hydrogen uptake is set to -50 mmol·gDW^{-1}hr^{-1}. Several interesting features are summarized. For OGOR, the curve shows multiple linear segments and therefore multiple phenotypes, as depicted in Fig. 5(b). In Fig. 5(f), when the flux of ferredoxin reductase reaches zero, the growth rate decreases to that of the CBB cycle only and rTCA is effectively shut off. This is reasonable because ferrodoxin is needed for the OGOR reaction in the rTCA cycle.

Alternative suboptimal growth mode

One interesting observation of the robustness study is that no

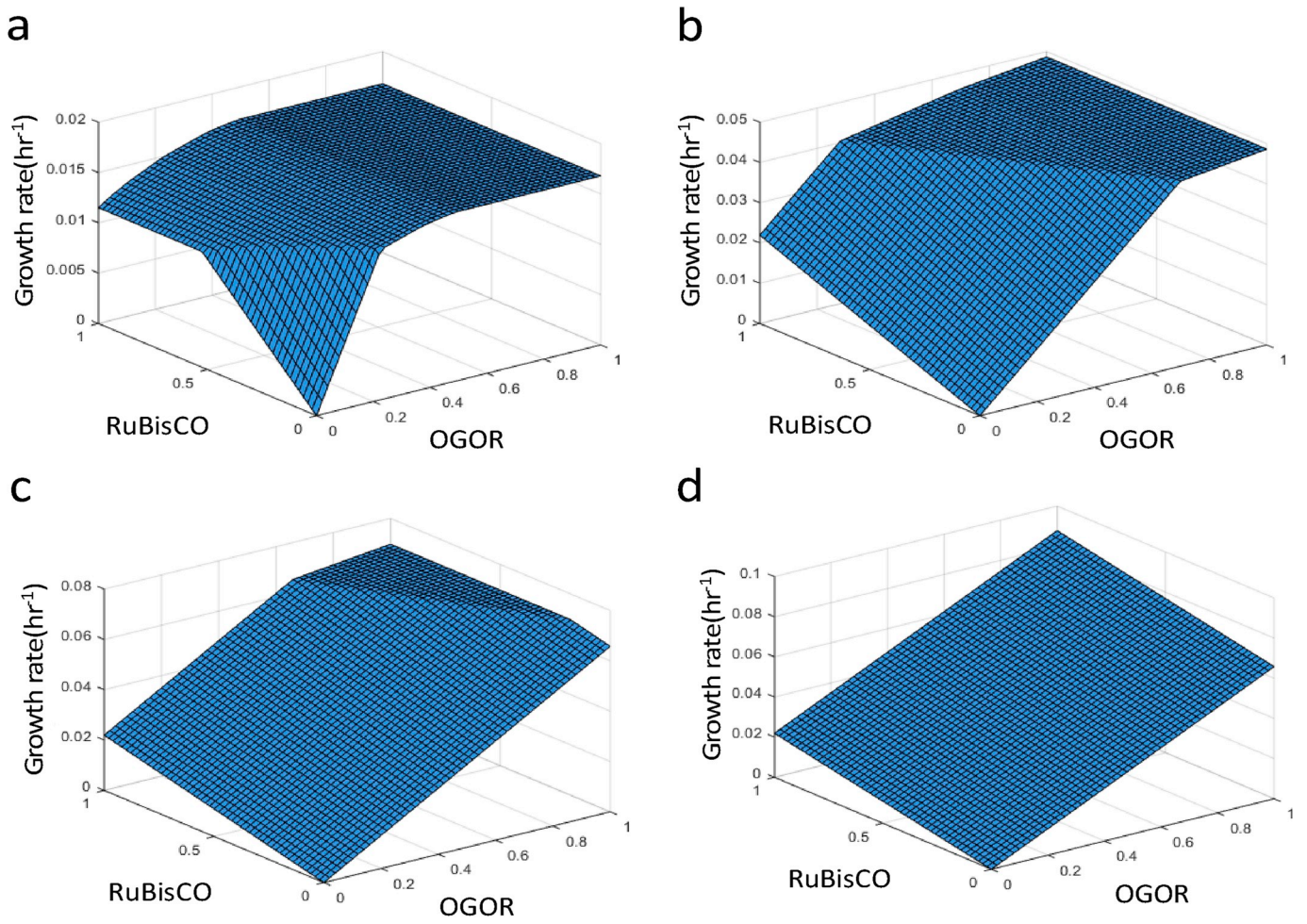

Fig. 4. Three-dimensional plot of growth rate as a function of OGOR and RuBisCO flux at various hydrogen uptake levels. (a) Hydrogen uptake = -8 mmol.gDW^{-1} hr^{-1}, (b) Hydrogen uptake = -13 mmol.gDW^{-1} hr^{-1}, (c) Hydrogen uptake = -17 mmol.gDW^{-1} hr^{-1}, (d) Hydrogen uptake = -50 mmol.gDW^{-1} hr^{-1}. All values shown are the lower bounds used in the computation. Abbreviations: OGOR, 2-oxoglutarate:ferredoxin oxidoreductase; RuBisCO, ribulose 1,5-bisphosphate carboxylase/oxygenase.

Table 1
Growth rate summary for single and dual carbon fixation for different enzyme capacity ratios and states. For the carbon-limited state, the results show that dual carbon fixation cycle enhances the growth rate. Growth rates of the dual cycle are higher than those of the single cycle. For the hydrogen-limited state, the dual cycle shows no growth rate enhancement. For the carbon-limited state, the lower bound of hydrogen uptake is set to -50 mmol.gDW^{-1}.hr^{-1}. For the hydrogen-limited state, the lower bound of hydrogen uptake is set to be -8 mmol.gDW^{-1}. hr^{-1}.

Enzyme capacity ratio(Rubisco:OGOR)					
Enzyme capacity(mmol/gDWhr)	Rubisco		1	3	1
	OGOR		1	1	3
Growth rate)(1/hr)	rTCA cycle	Carbon limited state	0.0658	0.0658	0.1364
	Calvin cycle		0.0219	0.0658	0.0219
	Dual cycle		0.0877	0.1316	0.1592
	rTCA cycle	Hydrogen limited state	0.0168	0.0168	0.0168
	Calvin cycle		0.0115	0.0115	0.0115
	Dual cycle		0.0168	0.0168	0.0168

knockout of the single heterologous enzyme in the simulation is lethal (Fig. 5). (To simulate the knockout of any enzyme, the corresponding reaction or reactions can simply be constrained to carry zero flux. By setting both the upper and lower bounds of a reaction to 0 mmol.gDW^{-1} hr^{-1}, a reaction is essentially knocked out, and is restricted from carrying flux.) This prompts us to perform a series of multiple enzyme knockout in the simulation to determine the viability and identify alternative suboptimal growth modes. The result is shown in Fig. 6. As a comparison, Fig. 6(a) shows a typical scenario of rTCA cycle, in which four carboxylating enzymes (POR, OGOR, isocitrate dehydrogenase, and phosphoenolpyruvate carboxylase) fix CO_2 and acetyl-CoA serves as the cycle product. There is one important caveat as we progressively remove heterologous enzymes in various combinations. When POR is knocked out, the glyoxylate shunt starts to emerge as shown in Fig. 6(b). When ACL is further removed, the strain shows viability (Fig. 6(c)). As the ACL reaction that provides a route to complete the rTCA cycle is removed, we expect complete disruption of the rTCA cycle because of its removal. The flux balance analysis result is somewhat surprising. Most flux (> 10% of the upperbound flux of OGOR) is concentrated on a cycle of four metabolites comprising

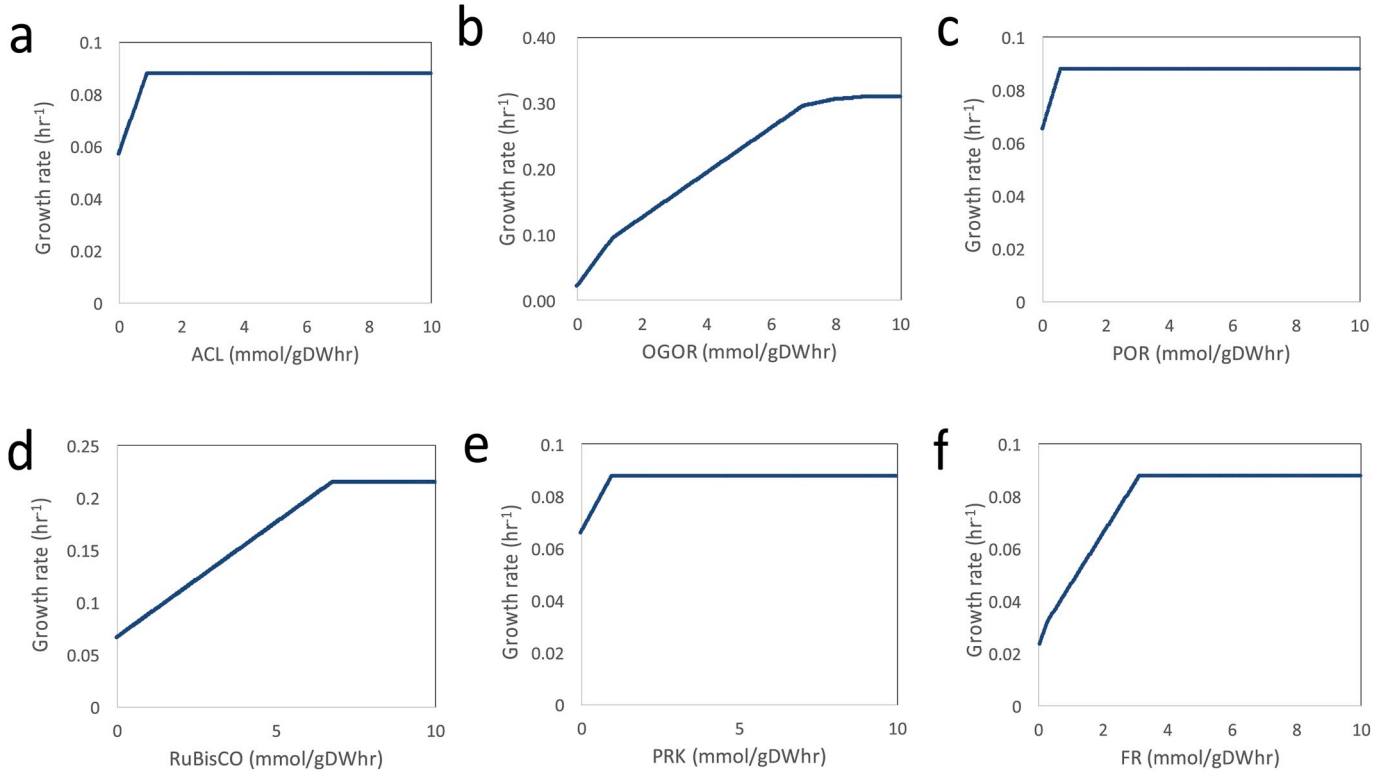

Fig. 5. Robustness analysis for maximum growth rate while varying flux through different enzymes. (a) ACL, (b) OGOR, (c) POR, (d)RuBisCO, (d) PRK (f) FR. Abbreviations: ACL, ATP citrate lyase; OGOR, 2-oxoglutarate:ferredoxin oxidoreductase; POR, pyruvate oxidoreductase; RuBisCO, ribulose 1,5-bisphosphate carboxylase/oxygenase; PRK, phosphoribulokinase; FR, favin reductase.

succinate, isocitrate, succinyl-CoA and 2-ketoglutarate. The flux map in Fig. 6(c) is replotted in Fig. 6(d) to highlight that the four-metabolite cycle stands out and is no longer embedded within the rTCA cycle and the remaining enzymes in the existing TCA cycle play a role in completing the replenishment of intermediates drained for biosynthesis of biomass. Such a carbon fixation cycle is a metabolic shortcut of rTCA cycle and the enzyme isocitrate lyase bypasses the remaining rTCA cycle [5]. Moreover, one important feature is that glyxolate, a C2 compound, emerges as the only product of the carbon fixation cycle. Here for the first time, we demonstrate its seamless integration with existing core metabolism of *E. coli*. We also find that one heterologous enzyme (OGOR) alone in the central metabolism will convert *E. coli* to grow *in silico* with such a four metabolite cycle.

Discussion

We have successfully constructed an *in silico* strain that can assimilate CO_2 using hydrogen for energy with dual carbon fixation cycles. By inserting heterologous enzymes, *E. coli*, a normally obligate heterotroph, is converted to a chemolithotroph using both inorganic carbon and energy source for growth. In terms of electron uptake and ATP generation, our strain is similar to chemolithotrophs such as hydrogen bacteria. These bacteria generate ATP by transporting electrons from reduced forms of the inorganic compound to a terminal electron acceptor. In heterotrophic growth, organic carbon sources such as glucose are supplied for growth as both a carbon and energy source. In our strain, the inorganic carbon source (in our case, CO_2) is decoupled from the energy source (hydrogen). The decoupling makes it possible to use their uptake as an independent parameter to profile the autotrophic growth. Indeed, when we vary the hydrogen (energy source) uptake, we discover that the strain shows hierarchy of usage of carbon fixation cycle and two distinct states – carbon-limited and energy-limited. With both cycles running to assimilate CO_2, it is possible to enhance growth rates provided that hydrogen is amply supplied.

Another implication is that only a few heterologous enzymes are needed to enable *E. coli* to grow autotrophically. Such a conclusion again shows the plasticity of metabolism and seems to be conceptually consistent with a recent finding that only five mutations are needed to create a non-native CBB cycle [13]. This point is most evident in the caveat that we find as we progressively remove heterologous enzymes. We find that one heterologous enzyme (OGOR) alone in the central metabolism will enable *E. coli* to grow with a four-metabolite cycle as depicted in Fig. 6(d). In other words, a previously-proposed short carbon fixation cycle [5], comprising only four metabolites, is seamlessly integrated. Such a cycle is a metabolic shortcut of rTCA cycle.

Finally, we comment on the experimental realization of our strain using a synthetic biology approach. One underlying assumption for constraint-based flux balance analysis is to use biomass as an objective and maximize the growth rate. Such flux balance analysis identifies key enzymes for such metabolic rewiring and provides the genetic basis for rational metabolic engineering design. However, if one naively heterologously expresses the enzymes, one cannot expect to achieve optimized growth on the first attempt. Because our model does not account for kinetic or regulation effects, a finely-tuned flux distribution might be required to balance the rate of sugar uptake by biosynthetic pathways branching from the CBB cycle with the rate of sugar biosynthesis from CO_2 fixation. The kinetic requirements of such a balance are detailed in recent theoretical analysis [12]. Laboratory evolution in a specially-designed bioreactor with a hydrogen gaseous environment [29] may provide a route to explore such multivariate fine-tuning required for operating such a non-native cycle.

Author contribution

CCH and SCL contributed to conceptulation and analysis of the data. HTYC and YTY. contributed to the computation, analysis of the data,

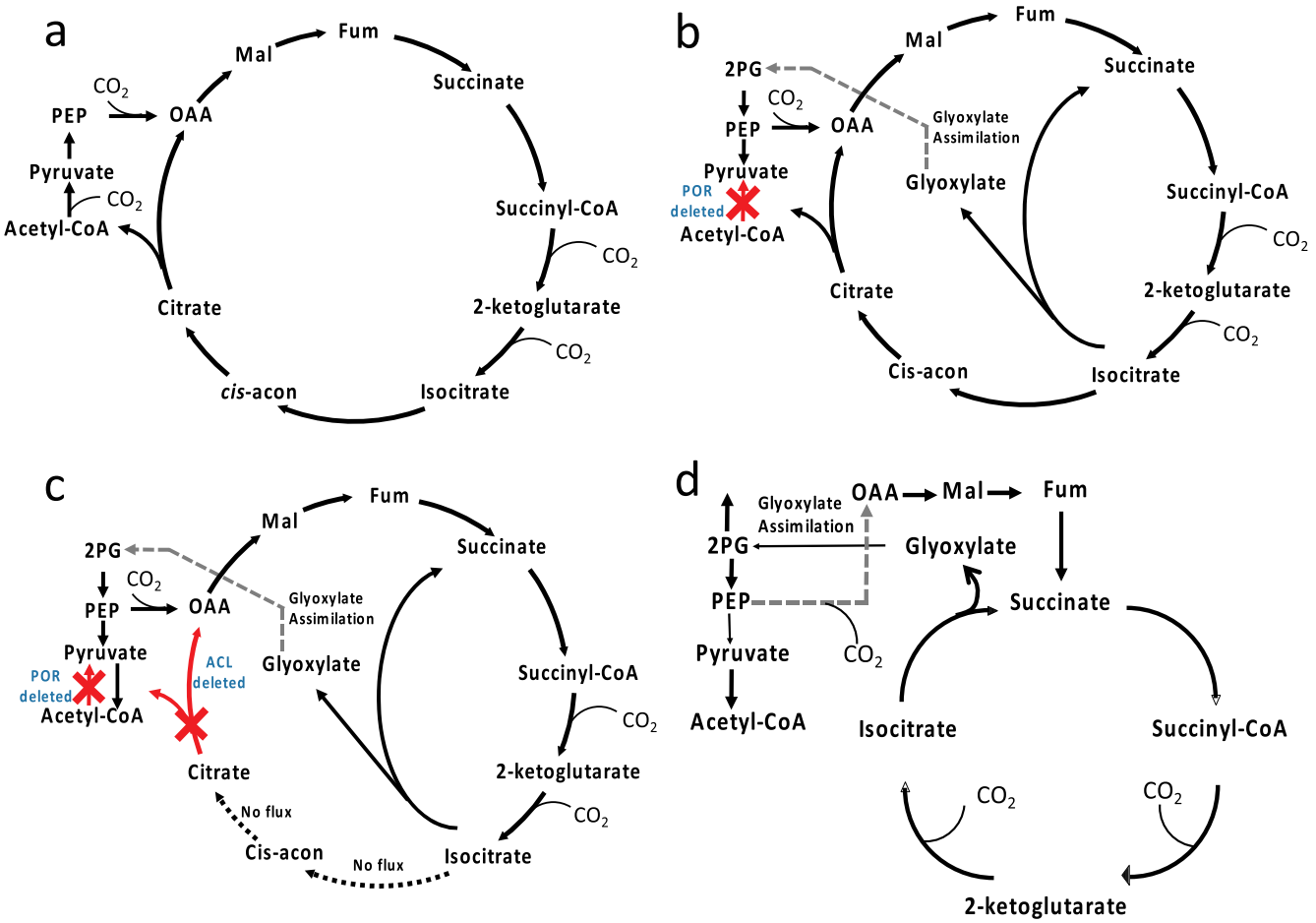

Fig. 6. Alternative scenario of flux of the rTCA cycle. (a) rTCA cycle flux when the full TCA cycle is reversed with acetyl-CoA as the cycle product. (b) rTCA cycle flux with glyoxylate shunt with POR enzyme knocked out. Part of the flux goes through the glyoxylate shunt to bypass the rTCA cycle. Both glyoxylate and acetyl-CoA are cycle products. The red cross symbol (x) indicates that the corresponding enzyme is knocked out in the simulation. (c)Flux map when both POR and ACL are knocked out. The red cross symbol (x) indicates that the corresponding enzyme is knocked out in the simulation. The black dash arrows indicates no flux from Cis-acon to citrate and from isocitrate to cis-acon. (d) Replot of (c) to highlight a four-metabolite cycle comprising succinate, isocitrate, succinyl-CoA and 2-ketoglutarate. Part of the existing rTCA cycle serves as an anaplerotic reaction to replenish the intermediates of this four-metabolite cycle drained for biosynthesis. Glyoxylate serves as the only cycle product. Abbreviations: 2 PG, D-glycerate-2-phophate; Fum, fumarate; Mal, Malate; OAA, oxaloacetate; PEP, phosphoenolpyruvate; ACL, ATP citrate lyase; POR, pyruvate oxidoreductase. Cis-acon, cis-aconitate; OGOR, 2-oxoglutarate:ferredoxin oxidoreductase.

and manuscript writing and editing. TYH contributed to computation, supervision and fund acquisition.

Note

The authors declare no competing financial interests.

Acknowledgements

Y. T. Y. would like to acknowledge funding support from the Ministry of Science and Technology under grant numbers MOST 105-2221-E-007-130-MY3 and MOST 107-2621-M-007 -001 -MY3. C. C. H. would like to acknowledge funding support from the Ministry of Science and Technology under grant numbers MOST 107-2621-M-005 -007-MY3 and 107-2621-M-005-001.

References

[1] Normile D. Round and round: a guide to the carbon cycle. Science 2009;325:1642–3.
[2] Berg IA. Ecological aspects of the distribution of different autotrophic CO_2 fixation pathways. Appl Environ Microbiol 2011;77:1925–36.
[3] Berg IA, Kockelkorn D, Ramos-Vera WH, Say RF, Zarzycki J, Hügler M, Alber BE, Fuchs G. Autotrophic carbon fixation in archaea. Nat Rev Microbiol 2010;8:447–60.
[4] Erb TJ. Carboxylases in natural and synthetic microbial pathways. Appl Environ Microbiol 2011;77:8466–77.
[5] Bar-Even A, Noor E, Lewis NE, Milo R. Design and analysis of synthetic carbon fixation pathways. Proc Natl Acad Sci USA 2010;107:8889–94.
[6] Volpers M, Claassens NJ, Noor E, van der Oost J, de Vos WM, Kengen SWM, et al. Integrated *in Silico* analysis of pathway designs for synthetic photo-electro-autotrophy. PLoS One 2016;11(6):e0157851.
[7] Gong F, Liu G, Zhai X, Zhou J, Cai Z, Li Y. Quantitative analysis of an engineered CO_2-fixing Escherichia coli reveals great potential of heterotrophic CO_2 fixation. Biotechnol Biofuels 2015;8:86.
[8] Zhuang ZY, Li SY. RuBisCO-based engineered *Escherichia coli* for in situ carbon dioxide recycling. Bioresour Technol 2013;150:79–88.
[9] Guadalupe-Medina V, Wisselink HW, Luttik MA, de Hulster E, Daran JM, Pronk JT, van Maris AJ. Carbon dioxide fixation by Calvin-Cycle enzymes improves ethanol yield in yeast. Biotechnol Biofuels 2013;6:125.
[10] Antonovsky N, Gleizer S, Milo R. Engineering carbon fixation in E. coil: from heterologous RuBisCO expression to the Calvin-Benson-Bassham cycle. Curr Opin Biotechnol 2017;47:83–91.
[11] Antonovsky N, Gleizer S, Noor E, Zohar Y, Herz E, Barenholz U, Zelcbuch L, Amram S, Wides A, Tepper N, Davidi D, Bar-On Y, Bareia T, Wernick DG, Shani I, Malitsky S, Jona G, Bar-Even A, Milo R. Sugar synthesis from CO_2 in *Escherichia coli*. Cell 2016;166:115–25.
[12] Barenholz, et al. Design principles of autocatalytic cycles constrain enzyme kinetics and force low substrate saturation at flux branch points. eLife 2017;6:e20667https://doi.org/10.7554/eLife.20667.
[13] Herz E, Antonovsky N, Bar-On Y, et al. The genetic basis for the adaptation of E-coli to sugar synthesis from CO_2. Nat Commun 2017;8:1705.

[14] Schwander Thomas, von Borzyskowski Lennart Schada, Burgener Simon, Cortina Niña Socorro, Erb Tobias J. A synthetic pathway for the fixation of carbon dioxide in vitro Science. 2016 Nov 18 vol. 354. 2016. p. 900–4. 6314.
[15] Tcherkez GGB, Farquhar GD, Andrews TJ. Despite slow catalysis and confused substrate specificity, all ribulose bisphosphate carboxylasesmay be nearly perfectly optimized. Proc Natl Acad Sci USA 2006;103:7246–51.
[16] Savira Y, Noor E, Milo R, Tlusty T. Cross-species analysis traces adaptation of RuBisCO toward optimality in a low-dimensional landscape. Proc Natl Acad Sci USA 2010;107:3475–80.
[17] Bar-Even A, Flamholz A, Noor E, Milo R. Thermodynamic constraints shape the structure of carbon fixation pathways. Biochim Biophys Acta 2012;1817:1646–59.
[18] Sawers RG, Ballantine SP, Boxer DH. Differential expression of hydrogenase isoenzymes in *Escherichia coli K-12*: evidence for a third isoenzyme. J Bacteriol 1985;164:1324–31.
[19] Liu C, Colon BC, Ziesack M, Silver PA, Nocera DG. Water splitting-biosynthetic system with CO_2 reduction efficiencies exceeding photosynthesis. Science 2016;352:1210–3.
[20] Orth JD, Thiele I, Palsson BØ. What is flux balance analysis. Nat Biotechnol 2010;28:245–8.
[21] Palsson BØ. System biology: properties of reconstructed networks. New York: Cambridge University Press; 2011.
[22] Orth J, Fleming R, Palsson B. Reconstruction and use of microbial metabolic networks: the core Escherichia coli metabolic model as an educational guide. EcoSal Plus 2010. https://doi.org/10.1128/ecosalplus.10.2.1. 2010.
[23] Cromartie TH, Walsh CT. Escherichia coli glyoxalate carboligase. Properties and reconstitution with 5-deazaFAD and 1,5-dihydrodeazaFADH2. J Biol Chem 1976;251:329–33.
[24] Neidhardt FC, Ingraham JL, Schaechter M. Physiology of the bacterial cell: a molecular approach. Sinauer Associates; 1990.
[25] Spaans SK, Weusthuis RA, van der Oost J, Kengen SWM. NADPH-generating systems in bacteria and archaea. Front Microbiol 2015;6:742. https://doi.org/10.3389/fmicb.2015.00742.
[26] Steuber J, Krebs W, Bott M, Dimroth P. A Membrane-Bound NAD(P)(+)-Reducing hydrogenase provides reduced pyridine nucleotides during citrate fermentation by *Klebsiella pneumoniae*. J Bacteriol 1999;181:241–5.
[27] Schmitz O, Boison G, Salzmann H, Bothe H, Schutz K, Wang S-H, et al. HoxE–a subunit specific for the pentameric bidirectional hydrogenase complex (HoxEFUYH) of cyanobacteria. Biochim Biophys Acta 2002;1554:66–74. https://doi.org/10.1016/S0005-2728(02)00214-1.
[28] Wells MA, Mercer J, Mott RA, Pereira-Medrano AG, Burja AM, Radianingtyas H, et al. Engineering a non-native hydrogen production pathway into *Escherichia coli* via a cyanobacterial [NiFe] hydrogenase. Metab Eng 2011;13:445–53.
[29] Pilizota T, Yang Y-T. "Do it yourself" microbial cultivation techniques for synthetic and systems biology: cheap, fun, and flexible. Front Microbiol 2018;9:1666.